J Physiol (2003), **551.2**, *pp.* 403–417
DOI: 10.1113/jphysiol.2003.041723
www.jphysiol.org

Journal of Physiology

Ca^{2+}-independent, but voltage- and activity-dependent regulation of the NMDA receptor outward K^+ current in mouse cortical neurons

Tomomi Ichinose*, Shun Yu†, Xue Qing Wang*† and Shan Ping Yu*†

**Department of Neurology and Center for the Study of Nervous System Injury, School of Medicine, Washington University, St Louis, MO and †Department of Pharmaceutical Sciences, Medical University of South Carolina, SC, USA*

To test the novel hypothesis that the K^+ efflux mediated by NMDA receptors might be regulated differently than the influx of Ca^{2+} and Na^+ through the same receptor channels, NMDA receptor whole-cell currents carried concurrently or individually by Ca^{2+}, Na^+ and K^+ were analysed in cultured mouse cortical neurons. In contrast to the NMDA inward current carried by Ca^{2+} and Na^+, the NMDA receptor outward K^+ current or NMDA-K current, recorded either in the presence or absence of extracellular Ca^{2+} and Na^+, and at different or the same membrane potentials, showed much less sensitivity to alterations in intracellular Ca^{2+} concentration and underwent little rundown. In line with a selective regulation of the NMDA receptor K^+ permeability, the ratio of the NMDA inward/outward currents decreased, and the reversal potential of composite NMDA currents recorded in physiological solutions shifted by −8.5 mV after repeated activation of NMDA receptors. Moreover, a depolarizing pre-pulse of a few seconds or a burst of brief depolarizing pulses selectively augmented the subsequent NMDA-K current, but not the NMDA inward current. On the other hand, a hyperpolarizing pre-pulse showed the opposite effect of reducing the NMDA-K current. The voltage- and activity-dependent regulation of the NMDA-K current did not require the existence of extracellular Ca^{2+} or Ca^{2+} influx; it was, however, affected by the duration of the pre-pulse and was subject to a time-dependent decay. The burst of excitatory activity revealed a lasting upregulation of the NMDA-K current even 5 s after termination of the pre-pulses. Our data reveal a selective regulation of the NMDA receptor K^+ permeability and represent a novel model of voltage- and excitatory activity-dependent plasticity at the receptor level.

(Resubmitted 17 February 2003; accepted after revision 9 June 2003; first published online 14 July 2003)
Corresponding author S. P. Yu: Department of Pharmaceutical Sciences, College of Pharmacy, Medical University of South Carolina, 280 Calhoun Street, PO Box 250140, Charleston, SC 29425, USA. Email: yusp@musc.edu

L-Glutamate is the major excitatory neurotransmitter in the CNS (Watkins & Evans, 1981; Mayer & Westbrook, 1987*a*; Hollmann & Heinemann, 1994). Excessive glutamate release may cause neuronal cell death in brain disorders (Rothman & Olney, 1986; Choi, 1992). The ionotropic glutamate receptors (NMDA, AMPA and kainate receptors) contain integral cationic channels (Watkins & Evans, 1981; Mayer & Westbrook, 1987*b*; Ozawa *et al.* 1988; Monaghan *et al.* 1989). Considerable attention has been centred upon NMDA receptors because of their important roles in synaptic plasticity and other aspects of synaptic transmission, and because of their characteristic features, including high Ca^{2+} permeability, multiple modulatory sites and a unique voltage-dependent blockage by Mg^{2+} (Mayer *et al.* 1984, 1989; MacDermott *et al.* 1986; Gibb & Colquhoun, 1992).

Emerging evidence supports the idea that excessive K^+ efflux and intracellular K^+ depletion are key steps in cell shrinkage, cytochrome c release, caspase cleavage, endonuclease activation and apoptosis (Inai *et al.* 1997; McCarthy, 1997; Yu *et al.* 1997, 1999*b*; Dallaporta *et al.* 1998; Bortner & Cidlowski, 1999; Yu, 2003). Pro-apoptotic K^+ efflux can be mediated by voltage-gated K^+ channels (Yu *et al.* 1997) and by ionotropic glutamate receptor channels (Yu *et al.* 1999*a*; Xiao, *et al.* 2001). Although the K^+ permeability of NMDA receptors has been reported previously (MacDermott *et al.* 1986; Mayer & Westbrook, 1987*b*; Ascher & Nowak, 1988), much less is known about the characteristics of this permeability than about the NMDA receptor-mediated inward currents carried by Ca^{2+} and Na^+. In general, it is casually assumed that K^+ efflux is under the same regulation as for the influx of Ca^{2+} and Na^+. On the other hand, the profound differences in Ca^{2+} permeability associated with distinct NMDA receptor subunits and receptor mutations suggest that the permeability of an individual ion can be selectively altered (Burnashev *et al.* 1992; Schneggenburger, 1998). A

T. Ichinose and S. Yu contributed equally to this work.

study on a mutant NMDA receptor channel revealed further that upon activation, the NMDA receptor channel went through two conductance states of different selectivities for Na^+ and Cs^+ (Schneggenburger & Ascher, 1997). This observation implies that in addition to Ca^{2+}, the permeability of NMDA receptors to other cations might also be individually changed. The fact that NMDA receptor channels are homologous to voltage-gated K^+ channels (Wood *et al.* 1995; Niethammer *et al.* 1996; Tikhonov *et al.* 1999) implies further that the permeability of NMDA receptor to K^+ may have a common root with the voltage-gated K^+ channels, and may be regulated by a distinguishable mechanism. In the present study, the K^+-efflux-generated NMDA-K current ($I_{NMDA\text{-}K}$) was either isolated using Ca^{2+}-free and/or Na^+-free extracellular solutions, or studied as the outward current in the presence of physiological concentrations of Ca^{2+}, Na^+ and K^+. Our data indicate that the K^+ efflux via NMDA receptor channels is under a distinctive Ca^{2+}-independent regulation and is controlled by a novel mechanism of receptor plasticity. Some of the results of this work have been reported previously in the form of two abstracts (Yu & Ichinose, 1999; Ichinose & Yu, 2000).

METHODS

Cortical neuronal culture

Cortical cultures containing neurons and glia were prepared as described previously (Yu *et al.* 1999*b*). Briefly, dissociated cortical neurons of fetal mice from 15 to 17 days of gestation were plated onto a pre-established glial monolayer at a density of 3.5–4.0 hemispheres $(10\ ml)^{-1}$ in glass-bottomed 35 mm dishes (Falcon, Primaria), in Eagle's minimal essential medium (MEM, Earle's salts) containing 25 mM glucose, 5 % fetal bovine serum (FBS) and 5 % horse serum (HS). The medium was changed after 1 week to MEM containing 25 mM glucose and 10 % HS, as well as 10 μM cytosine arabinoside. Cultures were kept in a humidified incubator at 37 °C, in a 5 % CO_2 atmosphere. The glial bed was prepared from dissociated neocortices of postnatal day 1–3 mice, in Eagle's MEM containing 25 mM glucose, 10 % FBS, 10 % HS and 10 ng ml^{-1} epidermal growth factor; a confluent glial bed was formed in 1–2 weeks. Experiments were performed routinely on 12- to 15-day-old neurons, *in vitro*.

Animals were handled in accordance with a protocol approved by the institutional animal care committee. The pregnant mice were anaesthetized by inhaled halothane until breathing ceased. Pups were removed and decapitated immediately using standard sterile techniques. The mother mice were then killed by overdose of halothane.

Whole-cell recording of NMDA receptor currents

A 35 mm dish containing cortical cultures was placed on the stage of an inverted microscope, and membrane currents were recorded by whole-cell recording using an EPC-9 amplifier (List-Electronic, Germany). Spherical or near-spherical cells were chosen for the recording. Recording electrodes with a tip resistance of 5–8 MΩ (fire-polished; i.d. ~ 1–1.5 μm) were pulled from Corning Kovar Sealing no. 7052 glass pipettes (PG52151–4, WPI, USA), with the aid of a Flaming-Brown micropipette puller (P-80/PC, Sutter Instrument, USA). Achievement of adequate voltage clamp and space clamp under similar conditions has been demonstrated before (Wilson & Goldner, 1975). The offset potential of the recording pipette was routinely corrected to 0 mV after immersing the tip into the bath medium. This potential was checked at the end of experiments (usually 0–2 mV) and corrected if necessary. Recordings with a potential drift of more than 3 mV were discarded. A gigaseal with a resistance of 10–50 GΩ was formed before establishing the whole-cell recording mode. Series resistance compensation (40–60 %) was monitored and applied routinely during recordings. Current and voltage traces were displayed on a computer monitor and collected by the PULSE data acquisition/analysis software for off-line analysis; data analysis was performed using the PULSE/PULSEFIT software package (HEKE, Lambrect, Germany). Currents were digitally sampled at 50 μs (20 kHz) and filtered at 3 kHz by a three-pole Bessel filter. The culture dish being used for recording was continuously perfused by gravity at a rate of ~0.2 ml min^{-1}. The perfusion rate could be accelerated to replace the bath medium (< 0.5 ml in the central pool) in a few seconds, which was used for solution changes and drug application. NMDA was applied locally using a drug-delivery device, as described below.

To record the isolated outward NMDA-K current, the extracellular solution contained 120 mM *N*-methyl-D-glucamine (NMDG), 3 mM KCl, 1 mM $MgCl_2$ or 2 mM $CaCl_2$, 10 mM Hepes, 10 mM D-glucose and 0.5 μM tetrodotoxin (TTX). The osmolarity (~ 300 mosmol l^{-1}) and pH value (7.3) were adjusted with a solution of HCl. The electrode solution contained 120 mM CsCl or KCl, 2 mM Na_2-ATP or Mg-ATP, 0, 2 or 5 mM BAPTA, 10 mM tetraethylammonium (TEA) and 10 mM Hepes. Based on the fact that NMDA receptor channels are permeable to Cs^+, but voltage-gated K^+ channels are essentially not, Cs^+ and the pan K^+ channel blocker TEA were used in the internal solution to eliminate the current mediated by voltage-gated K^+ channels. TEA was added intracellularly to avoid its inhibitory effect on NMDA receptors from the outside of the membrane (Wright *et al.* 1991). To record composite NMDA currents, the external solution contained 120 mM NaCl, 3 or 5 mM KCl, 2 mM $CaCl_2$, 10 mM Hepes, 10 mM glucose and 0.5 μM TTX. The electrode solution for composite NMDA currents contained 120 mM CsCl or KCl, 2 mM Na_2-ATP, 0, 0.5 or 5 mM BAPTA and 10 mM Hepes. In some experiments, 2 μM Gd^{3+} or nifedipine was added to block voltage-gated Ca^{2+} channels; Gd^{3+} might additionally block stretch-activated channels. Some experiments used 10 mM BAPTA in internal solutions, and in experiments with thapsigargin, no BAPTA was added. When the concentration of K^+, Cs^+ or Na^+ was altered, the NMDG concentration in the solution was adjusted to maintain a consistent osmolarity. NMDA currents were evoked by local application of NMDA (100–200 μM) and glycine (10 μM) to the surface of the cell body using the DAD-12 drug delivery device (Adams & List, New York). The solution exchange time at the tip of the electrode was < 10 ms, as detected by the liquid junction potential; however, the real solution exchange around the neuron being recorded could be slower (⩾ 100 ms) depending on multiple factors including the location of the electrode, the shape and size of the neuron and the air pressure applied. In data analysis, the NMDA steady-state current was measured from the baseline level immediately before application of NMDA. All recordings were performed at room temperature (21 ± 1 °C) with a solution pH value of 7.35.

Statistical analysis

The Student's two-tailed *t* test was used for comparison of two experimental groups; the paired *t* test was applied to experiments

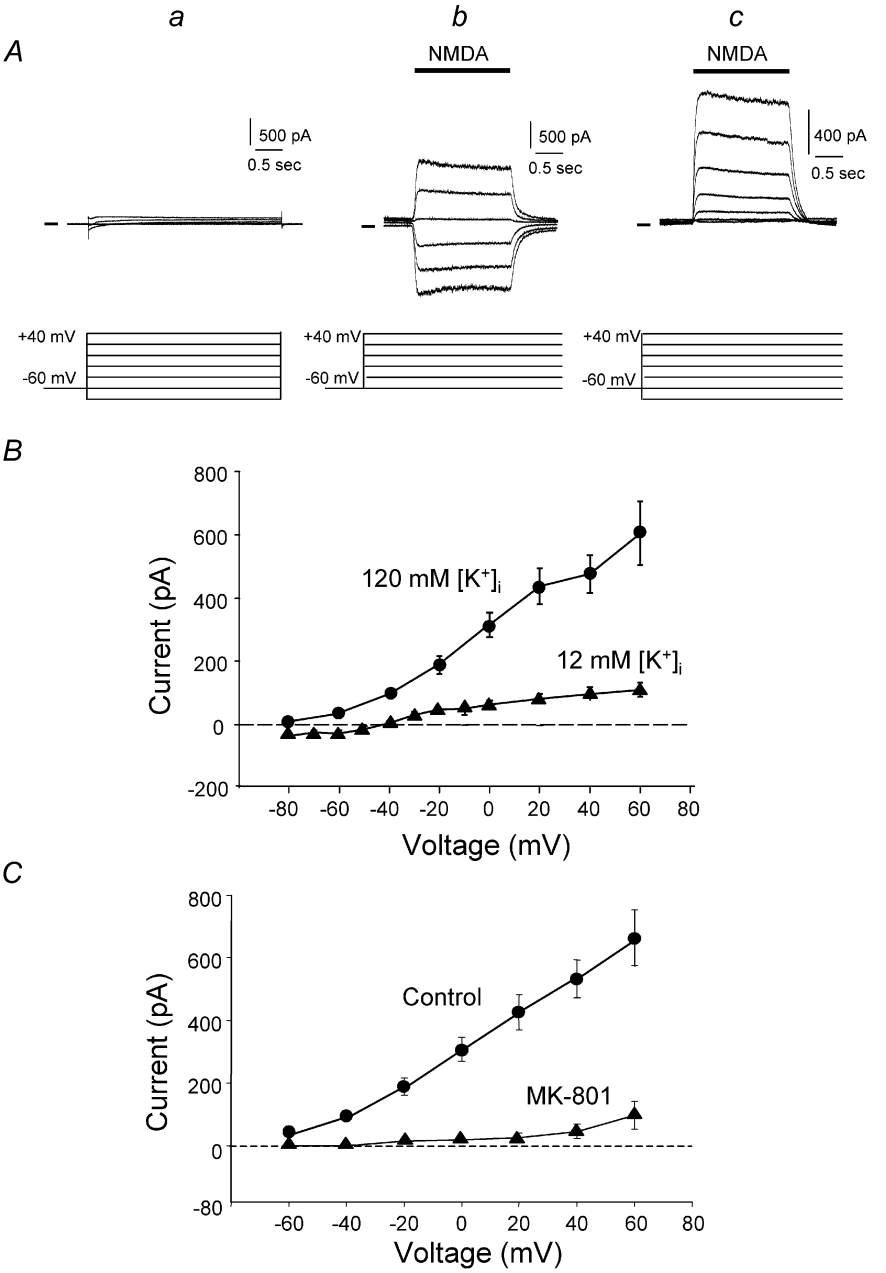

Figure 1. Composite NMDA currents and K⁺-efflux-carried NMDA outward current

Aa, voltage-activated membrane responses without NMDA application. The line drawing at the bottom illustrates the steps, starting points and ending points of the voltage changes. *b*, composite NMDA currents, I_{NMDA}, evoked by 100 μM NMDA plus 10 μM glycine in an external solution containing 120 mM Na^+, 2 mM Ca^{2+} and 5 mM K^+ (120 mM internal K^+). The current reversed at ~ 0 mV. *c*, NMDA (100 μM) and glycine (10 μM) evoked outward currents carried by K^+ efflux, $I_{NMDA\text{-}K}$, isolated by recording in a Ca^{2+}-free, Na^+-free external solution (substituted by NMDG) and 120 mM internal K^+. The currents had a negative reversal potential ~−80 mV. Current responses were evoked every 20 s and are superimposed. The short horizontal lines that appear before the current traces show the baseline level of the recordings. The voltage diagrams in *b* and *c* illustrate a 2 s delay between the voltage starting point and NMDA application; the returning of membrane potentials back to the holding potential is not shown. *B*, the sensitivity of $I_{NMDA\text{-}K}$ to intracellular K^+. At a low intracellular K^+ concentration of 12 mM, the reversal potential shifted to the right and $I_{NMDA\text{-}K}$ was largely eliminated ($n = 5$ cells for each point). *C*, $I_{NMDA\text{-}K}$ recorded in the Ca^{2+}-free and Na^+-free external solution was sensitive to block by MK-801 (10 μM, $n = 5$ for each group). The glycine antagonist 7-chlorokynurenic acid (10 M) also blocked the current ($n = 5$; data not shown).

with self-controls. Multiple comparisons were performed using a one-way ANOVA test followed by a Tukey test for multiple pairwise tests. Changes were identified as significant if the P value was less than 0.05. Mean values are reported together with the standard error of the mean (S.E.M.).

RESULTS

NMDA receptor currents carried by Ca^{2+} or Na^+ influx, and/or K^+ efflux

In whole-cell recordings with normal concentrations of Ca^{2+}, Na^+ and K^+ in external and internal solutions, 100 or 200 μM NMDA plus 10 μM glycine triggered the widely reported NMDA current, I_{NMDA}. The reversal potential of this current was around 0 mV, consistent with the multiple cation permeability of NMDA receptor channels (Mayer & Westbrook, 1987*b*; Fig. 1*A*). To isolate the current generated by K^+ efflux, NMDA was applied in a Ca^{2+}-free and Na^+-free extracellular solution. By thus eliminating Ca^{2+} and Na^+ influx, NMDA receptor activation generated outward currents even at negative membrane potentials (Fig. 1*A*). As expected for a K^+-mediated current, the outward $I_{NMDA\text{-}K}$ had a reversal potential of -86 ± 4 mV ($n = 8$); the reversal potential was shifted towards more depolarized levels when the intracellular K^+ concentration decreased (Fig. 1*B*) or the extracellular K^+ concentration increased (data not shown). As expected for a NMDA receptor-mediated current, the outward current was abolished by the NMDA receptor

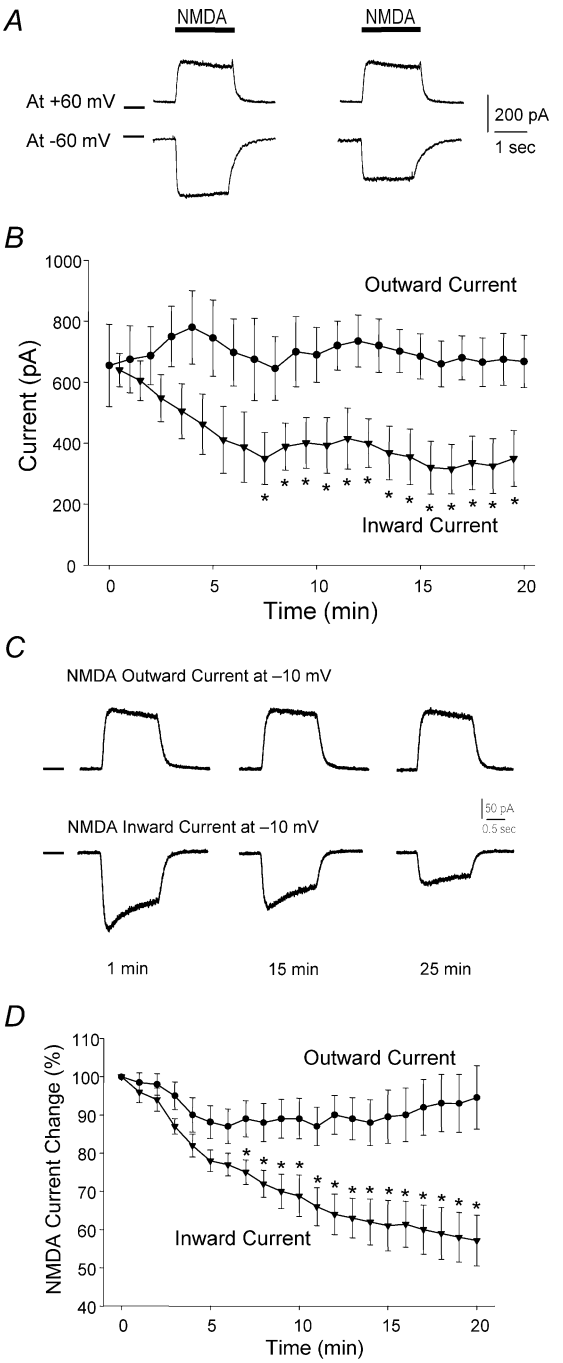

Figure 2. Different Ca^{2+} sensitivity of inward and outward NMDA currents under physiological conditions

A and *B*, NMDA outward and inward currents were recorded at +60 and −60 mV alternately in the same cells in the presence of physiological concentrations of extracellular and intracellular Ca^{2+}, Na^+ and K^+ (see Methods). No Ca^{2+} chelator was used. *A*, the NMDA inward current carried by the influx of Ca^{2+} and Na^+ showed time-dependent rundown, meanwhile the outward current generated by K^+ efflux remained stable. *B*, time-dependent rundown of NMDA inward current and lack of rundown of NMDA outward current in the same cells. The time points of the two lines are not matched as a result of alternative recordings in these cells ($n = 7$). *C* and *D*, NMDA receptor inward and outward currents were activated every 5 min at −10 mV with and without extracellular Na^+, respectively. Ca^{2+} (2 mM) was presented in extracellular solutions in both recordings. *C*, the inward current gradually declined, while the outward current remained stable during 30 min recordings. *D*, rundown of NMDA inward and outward currents compared at the same membrane potential. In this experiment, both inward and outward currents showed about a 20–30 % reduction between the first and second NMDA stimulations; data shown in the figure were started from the second NMDA responses. Inward and outward currents were recorded in different cells. The short horizontal bars in *A* and *C* to the left of the current traces show the baseline level of the recordings ($n = 14$ and 12 for inward and outward currents, respectively). $^*P < 0.05$ compared with the time-matched outward current.

antagonist MK-801 (10 μM; Fig. 1*C*) or the glycine site antagonist 7-chlorokynurenic acid (10 μM; data not shown). In this report, $I_{NMDA\text{-}K}$ was isolated in either Ca^{2+}- and Na^+-free, or only Na^+-free external solutions, or was recorded as the outward current at positive potentials in normal external and internal solutions. As a control, we monitored the chord conductance of cells responding to a −20 mV pulse (50 ms) from the holding potential of −60 mV. The chord conductance was unchanged under our experimental conditions, even after repeated NMDA applications and various voltage steps used for constructing current–voltage (*I–V*) curves (e.g. 4.1 ± 1.4 nS and 3.9 ± 1.5 nS before and after NMDA and voltage protocols, respectively, $P > 0.05$, $n = 8$).

$I_{NMDA\text{-}K}$ is less sensitive to changes in Ca^{2+} influx and intracellular free Ca^{2+} ($[Ca^{2+}]_i$)

The inward I_{NMDA} carried by Ca^{2+} and Na^+ influx is well known for its downregulation (desensitization/inactivation) by increased $[Ca^{2+}]_i$ (Legendre *et al.* 1993; Medina *et al.* 1995; Rosenmund *et al.* 1995). In our experiment, a similar Ca^{2+}-dependent 'rundown' of I_{NMDA} evoked 1 min apart was observed during the 15–20 min recordings. Addition of 5 mM BAPTA in the internal solution prevented the rundown, while the inclusion of 1 μM thapsigargin facilitated the rundown (data not shown). On the other hand, the isolated $I_{NMDA\text{-}K}$ was not sensitive to these manoeuvres; no rundown was observed regardless of the presence or absence of BAPTA and thapsigargin (e.g. the ratio for currents at 20 min/0 min = 0.97 ± 0.03, 1 μM thapsigargin and no BAPTA, $n = 5$). Furthermore, $I_{NMDA\text{-}K}$ remained stable even when 0.5 mM $CaCl_2$ was included in a BAPTA-free internal solution (current ratio for 20 min/0 min = 0.96 ± 0.06, $n = 3$).

The above experiments involving the inward and outward NMDA currents were performed in different extracellular solutions and different cells. To validate further the surprising Ca^{2+} insensitivity of the NMDA receptor K^+ permeability, the inward current carried by Ca^{2+} and Na^+ influx at negative potentials and the outward current carried by K^+ efflux at positive potentials were recorded

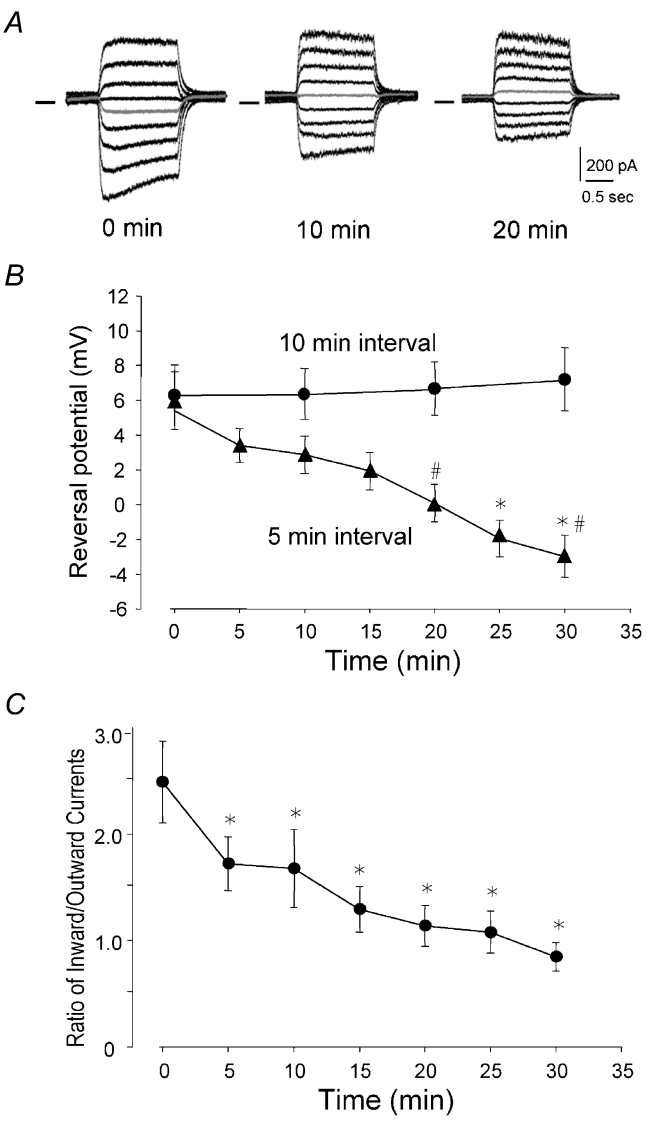

Figure 3. Time- and activation-dependent reversal potential shifts of composite NMDA currents in physiological solutions

The *I–V* relationship of composite NMDA receptor currents was recorded in regular internal and external solutions. *A*, the NMDA-stimulated responses at different potentials are superimposed and show a gradually declining inward conductance but stable outward conductance, recorded in the same neuron. NMDA receptor desensitization was seen as an outward rectification of the inward current recorded at 0 min; this desensitization diminished in subsequent responses. Meanwhile, rundown of the steady-state inward current was evident at later time points. Similar changes can be seen with inward currents in other figures. The grey line around the baseline area illustrates the reversal of the current direction, representing the negative shift of the reversal potential. NMDA inward and outward currents were evoked at potentials of −20 to +20 mV, in 5 mV increments. Voltage steps were separated by 9 s intervals; the intra-trial interval between complete *I–V* protocols was 5 min. Similar changes were observed when the *I–V* test was carried out in reverse (i.e. from +20 to −20 mV; data not shown, $n = 7$), suggesting that both protocols allowed sufficient $[Ca^{2+}]_i$ accumulation during the repetitive NMDA receptor activation. *B*, the line graph illustrates the gradual shift in the reversal potential from 5.4 to −3.2 mV when the *I–V* protocol was applied at 5 min intra-trial intervals. The reversal potential was unaltered when the interval was increased to 10 min. *C*, the ratio of NMDA inward and outward currents (inward/outward) recorded at −40 and +40 mV, respectively, gradually decreased during the 30 min recordings, consistent with the negative shift of the reversal potential ($n = 12$–14). * Significantly different from the controls at time 0 ($P < 0.05$ by ANOVA analysis); # significantly different from time-matched controls ($P < 0.05$ by *t* test).

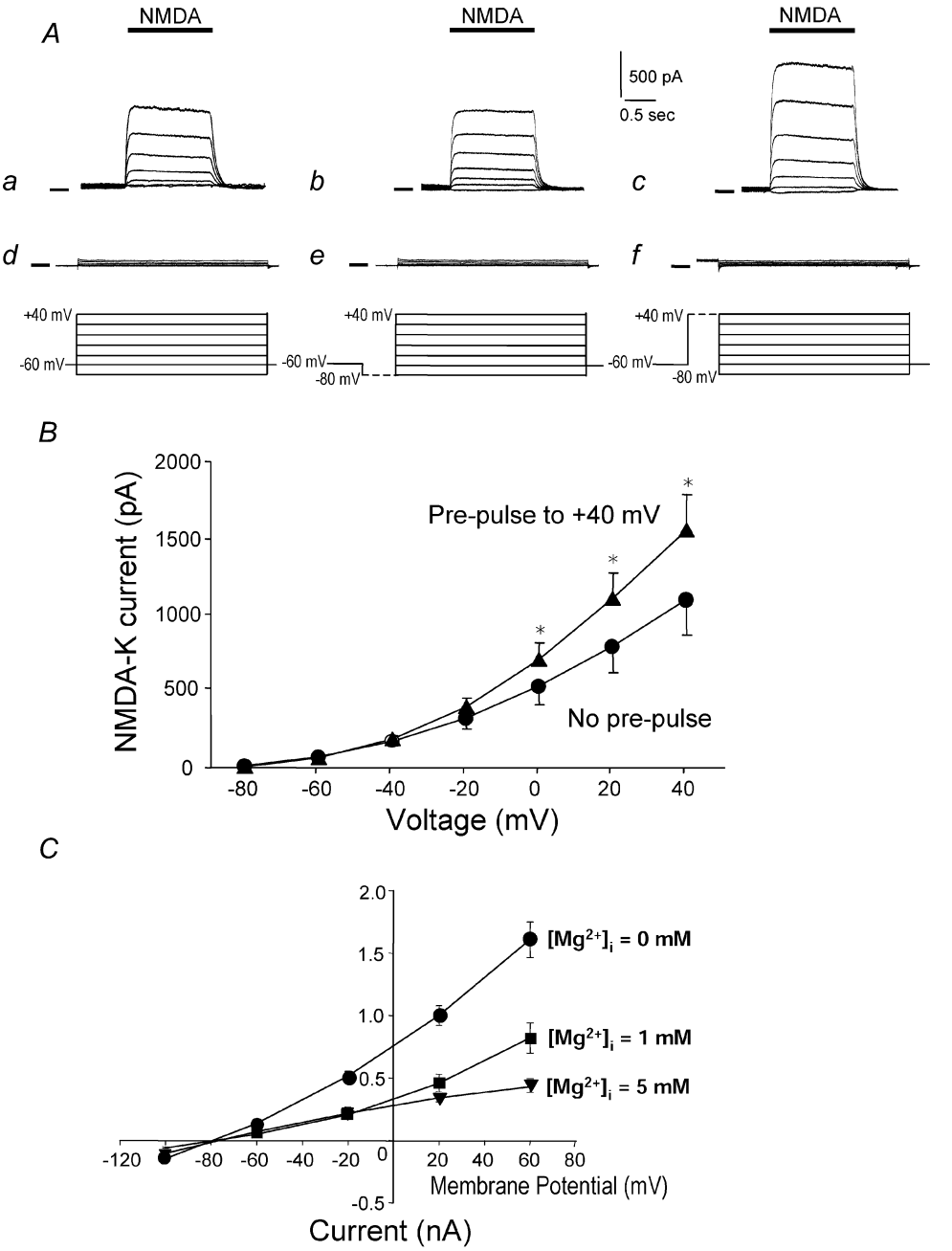

Figure 4. Selective regulation of I_{NMDA-K} by prior membrane potentials

A, the isolated I_{NMDA-K} was recorded at various membrane potentials using the Ca^{2+}-free, Na^{+}-free external solution containing 2 μM Gd^{3+} and 0.5 μM TTX; the Cs^{+}-based internal solution contained 10 mM TEA and 2 mM BAPTA (see Methods for other components in the solutions). *a*, control I_{NMDA-K} were evoked at membrane potentials from −80 to +40 mV at 20 mV increments; no pre-pulse was applied before NMDA application. Membrane responses to the same voltage jumps in the absence of NMDA applications are shown in *d*, and currents at different voltage levels are superimposed. The voltage protocol is illustrated in the line diagram below. In column *b*, each I_{NMDA-K} was evoked at different potentials following a hyperpolarizing pulse (10 s duration, represented by the dashed line) from a holding potential of −60 mV to −80 mV; this manipulation exerted no significant effect on I_{NMDA-K}. More hyperpolarizing pre-pulses were not tested. As shown in the line diagram below, there was a 1 s delay between the termination of the pre-pulse and the beginning of the NMDA application. Voltage-step-evoked membrane responses without NMDA application are shown in *e*. The I_{NMDA-K} shown in *c* were evoked 1 s after a depolarizing pre-pulse from −60 to +40 mV (10 s duration). I_{NMDA-K} was significantly enlarged following the pre-depolarization compared to the current generated without a pre-pulse or following a hyperpolarization. The voltage-step-triggered membrane responses in the absence of NMDA application are shown in *f*; the voltage protocol is illustrated at below the traces. The intra-trial interval between *I–V* protocols in the same cell was 1 min. The short horizontal lines before the current traces show the baseline of the recordings. Except for the dashed line, the voltage diagrams

alternately in the same cells and compared in the presence of physiological concentrations of Ca^{2+}, Na^+ and K^+. The membrane potential was held at −60 mV between NMDA applications. To allow Ca^{2+} accumulation in the intracellular space, no Ca^{2+} chelator was added to any solution. Under this condition, the NMDA-triggered inward current diminished gradually, whereas the $I_{NMDA\text{-}K}$, recorded a few seconds following each inward current in these cells, remained unchanged during the 20 min recording periods (Fig. 2).

It may be argued that even if the above experiments were performed in the same cells at the same extracellular Ca^{2+} concentration, the lack of rundown of the outward current could be attributable to a smaller Ca^{2+} influx during the NMDA application at the positive potential used for $I_{NMDA\text{-}K}$ recording. This argument, however, ignores the fact that $[Ca^{2+}]_i$ was cumulatively increased in these cells, as evidenced by the progressive decline of the NMDA inward current. To validate further the Ca^{2+} dependence of different NMDA currents, external Na^+ was substituted with NMDG to eliminate Na^+ influx. Using the normal and Na^+-free external solutions, we were able to record inward and outward NMDA currents, respectively, at an identical holding potential of −10 mV and at the same extracellular Ca^{2+} concentration of 2 mM. As shown in Fig. 2*C* and *D*, the inward NMDA current declined progressively during 20 min recordings, while the outward $I_{NMDA\text{-}K}$ remained relatively stable. The Na^+-free condition may increase the Ca^{2+} permeability (P_{Ca}) relative to that of Na^+ (P_{Na}), leading to an increased P_{Ca}/P_{Na} (Jatzke *et al.* 2002); this effect, however, appeared to have no impact on the $I_{NMDA\text{-}K}$ associated with K^+ permeability.

Should the individual ion permeability of NMDA receptors be differentially regulated, the reversal potential of composite currents is expected to alter accordingly. Confirming this prediction, the reversal potential of composite NMDA currents recorded in regular internal and external solutions indeed shifted towards negative values. After 20–30 min repeated NMDA receptor activations of an *I–V* protocol at 5 min intra-trial intervals, the reversal potential was shifted from 5.4 ± 1.1 to −3.2 ± 1.2 mV (−8.5 mV shift, $n = 14$, $P < 0.01$; Fig. 3*A* and *B*). In addition, the inward current gradually declined, while the outward current was relatively stable (Fig. 3*A*). As a result, the ratio of NMDA inward to outward currents (inward current/outward current) was reduced from 2.5 ± 0.4 to 0.8 ± 0.1 after 30 min recordings (Fig. 3*C*). The negative shift in the reversal potential was largely eliminated when 10 mM BAPTA was included in the internal solution; the reversal potential was 5.6 ± 1.0 and 2.1 ± 1.3 mV at the start and 30 min later, respectively (−3.5 mV shift, $P < 0.05$ compared with the −8.5 mV shift without BAPTA; $n = 7$). Moreover, extending the intra-trial interval to 10 min averted the reversal potential shift (Fig. 3*B*). Thus, these results are consistent with the notion that the downregulation of NMDA inward current mainly depends on Ca^{2+} influx and lasting $[Ca^{2+}]_i$ accumulation (Rosenmund & Westbrook, 1993), whereas $I_{NMDA\text{-}K}$ is insensitive to changes in $[Ca^{2+}]_i$.

NMDA receptor plasticity: a selective modulation of $I_{NMDA\text{-}K}$ by prior membrane potential and prior membrane excitatory activity

Transient and prolonged membrane depolarizations occur in physiological and pathological conditions. Since the NMDA receptor pore region exhibits high homology to voltage-gated K^+ channels, we speculated that this homology might be reflected in the behaviour of NMDA receptor K^+ permeability. Although NMDA receptor channels are not voltage-activated, a voltage-sensitive conformational change in the pore region might modify their K^+ conductance through the channels. As the first step to exploring this possibility, the sensitivity of $I_{NMDA\text{-}K}$ to prior membrane potentials was tested. In the *I–V* protocol for NMDA currents, each voltage step was preceded by a 10 s depolarizing or a hyperpolarizing pulse (from −60 to +40 mV or from −60 to −80 mV). Although the 20 mV hyperpolarization did not change the outward $I_{NMDA\text{-}K}$, the pre-depolarization augmented the current (27 ± 12 % increase for the current at +40 mV compared with that without a pre-pulse; $n = 6$, $P < 0.05$; Fig. 4*A*). The enhanced current created an augmented outward rectification in the *I–V* relationship (Fig. 4*B*). Conversely, switching the pre-potential from +40 to −80 mV before NMDA application diminished the enhancement of $I_{NMDA\text{-}K}$ (105 ± 13 % of the control current without a pre-pulse, $n = 8$, $P > 0.05$; and see Fig. 5*B*).

These experiments were performed in an internal solution containing 1 mM Mg^{2+}. Unlike the inward current, the outward $I_{NMDA\text{-}K}$ was blocked by Mg^{2+} even at positive potentials (Fig. 4*C*). The voltage-independent block by Mg^{2+} shown as a linear *I–V* curve confirmed that the enhancement of the NMDA outward current by pre-

at the bottom illustrate the actual time points at which the membrane potential was changed. The current traces represent similar results from six cells. *B*, effects of pre-depolarization on the *I–V* relationship of $I_{NMDA\text{-}K}$; same voltage protocol as shown in *Ac*. The depolarizing pre-pulse enhanced $I_{NMDA\text{-}K}$ and intensified the outward rectification compared with the currents recorded without a pre-pulse ($n = 10$ for each point). *$P < 0.05$ by paired *t* test for currents recorded in the same cells. *C*, internal Mg^{2+} blocked $I_{NMDA\text{-}K}$ in a concentration-dependent, but voltage-independent manner (shown as a straight line at 5 mM $[Mg^{2+}]_i$; $n = 20$–50 for each point). $P < 0.05$ compared with 0 mM Mg^{2+} controls at all points.

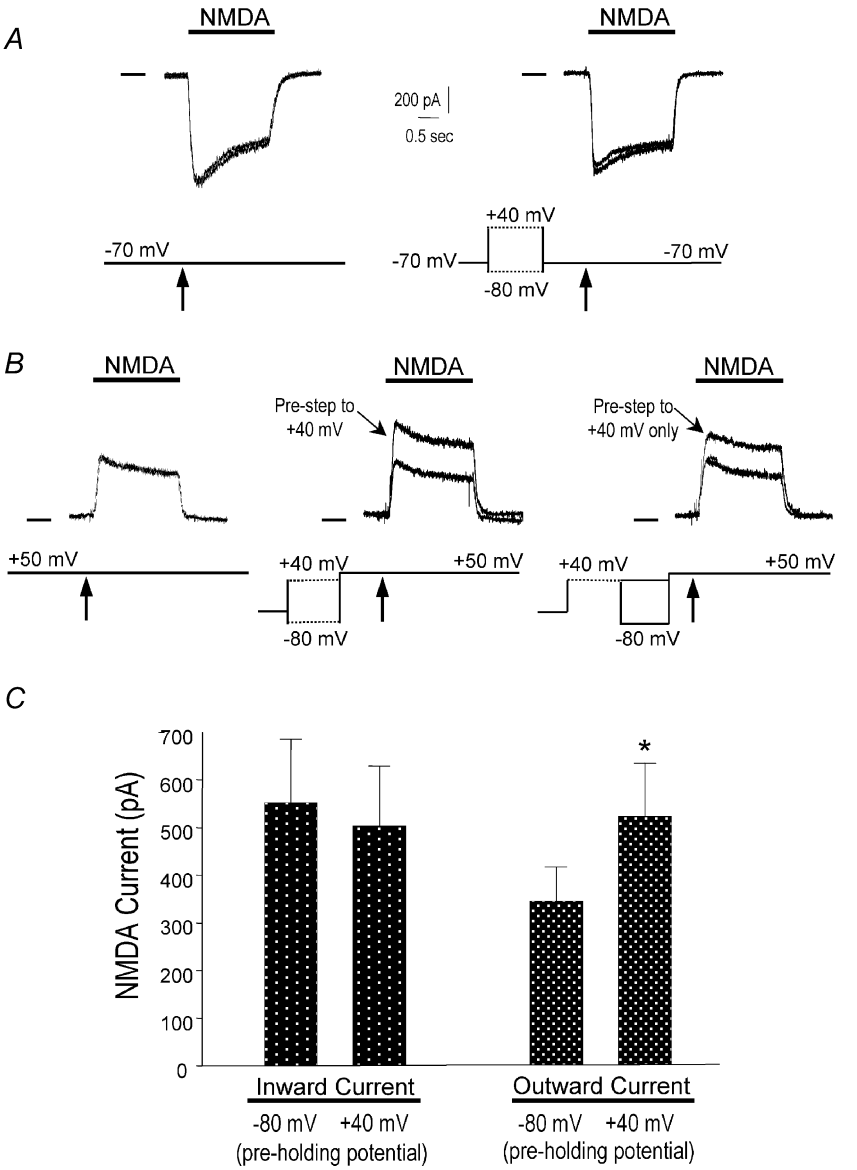

Figure 5. Voltage- and time-dependent selective upregulation of $I_{NMDA\text{-}K}$

NMDA inward and outward currents were recorded in a Mg^{2+}-free external solution containing physiological concentrations of Ca^{2+} and Na^{+}. Nifedipine (2 μM) and TTX (0.5 μM) were added into the external solution to block voltage-gated L-type Ca^{2+} channels and Na^{+} channels. To prevent activation of K^{+} channels, the K^{+}-free internal solution contained 120 mM Cs^{+} plus 10 mM TEA. *A*, the NMDA inward current carried by Ca^{2+} and Na^{+} influx was recorded at −70 mV; no change was detected when two currents were evoked with an interval of 1 min (left, two overlapping current traces). Pre-pulses to hyperpolarized (−80 mV) or depolarized (+40 mV) potentials completed 1 s before NMDA application did not alter the inward current (right, two overlapping current traces). The voltage protocol is shown under the current traces; the dotted line represents the 10 s duration of the pre-pulse. *B*, the NMDA outward current carried by Cs^{+} efflux was recorded at +50 mV in the external solution of normal Ca^{2+} and Na^{+}; without pre-pulses, two successive recordings evoked two similar currents (left, superimposed current traces). The two currents in the middle were recorded following pre-pulses to −80 and +40 mV. Although a pre-step to −80 mV did not affect the outward current, a pre-depolarization markedly enhanced the current. Briefly switching the membrane potential from +40 to −80 mV before NMDA application eliminated the depolarization-initiated upregulation of the NMDA outward current (right, overlapping currents). Arrows below the voltage protocol diagrams mark the time points for NMDA (100 μM) and glycine (10 μM) application. Recordings were made in the same solutions and from same cells. The effect of a pre-pulse to −80 mV was tested before stepping to +40 mV with 1 min separation; the interval between episodes was 1 min. *C*, the bar graph summarizes the data shown in *A*. The inward NMDA current recorded at −70 mV was almost identical, regardless of the pre-existing membrane potential; the outward current recorded at +50 mV, however, was enhanced following a pre-depolarization ($n = 7$). $^{*}P < 0.05$ compared with the current without a pre-pulse or that after a pulse to−80 mV.

depolarization was not the result of a diminished Mg^{2+} blockade at those membrane potentials.

To understand this selective modulation in more physiological Ca^{2+} and Na^{+} conditions, and to further rule out a role for Mg^{2+} in the modulation, the NMDA currents were recorded in the presence of normal external Ca^{2+} and Na^{+}, but with no Mg^{2+} in the external and internal solutions (see Fig. 1*A*). In addition, TEA (10 mM) and Cs^{+} (120 mM) were used in a K^{+}-free internal solution to eliminate K^{+} efflux through voltage-gated K^{+} channels. The Ca^{2+} channel antagonist nifedipine (2 μM) and the Na^{+} channel blocker TTX (0.5 μM) were added to the external solution to block major voltage-gated Ca^{2+} and Na^{+} channels in cortical neurons. Under this condition, the NMDA inward current at −70 mV and the outward current at +50 mV were stable when the same current was recorded 1 min later (Fig. 5*A* and *B*). The NMDA inward current was not affected by a pre-depolarization from −70 to +40 mV (10 s duration) that was complete 1 s before NMDA application (93 ± 6 % of controls, $n = 6$, $P > 0.05$) or a pre-hyperpolarization from −70 to −80 mV (99 ± 3 % of controls, $n = 6$, $P > 0.05$; Fig. 5*A*). The prior depolarization, however, did exert a marked enhancing effect on the NMDA outward current (53 ± 9 % increase compared with the current without a pre-pulse, $n = 7$, $P < 0.01$; Fig. 5*B*). This depolarization-induced delayed upregulation of the NMDA outward current was abolished by a hyperpolarizing pulse from +40 to −80 mV before NMDA application (Fig. 5*B*), suggesting a downregulation by hyperpolarization. The selective upregulation of the NMDA outward current in the absence of Mg^{2+} further ruled out the possibility that relief of the Mg^{2+} blockade underlay this modulation.

More experiments were performed on the isolated $I_{NMDA\text{-}K}$ using the Ca^{2+}-free and Na^{+}-free external solution. Equal voltage steps in opposite directions (from 0 to either −50 or +50 mV) were applied alternately before recording the currents at 0 mV. $I_{NMDA\text{-}K}$ increased following a pre-pulse to +50 mV (35 ± 11 % increase compared with currents without pre-pulse, $n = 5$, $P < 0.05$), and decreased following a pre-hyperpolarization to −50 mV (27 ± 8 % reduction, $n = 5$, $P < 0.05$). This experiment with equal voltage steps of opposite polarities excluded the possibility that the change in NMDA receptor behaviour was induced by the asymmetrical voltage steps used in some experiments.

The voltage 'pre-conditioning' effects on NMDA receptors might be regarded as a model of 'receptor plasticity'. This receptor plasticity, like the plasticity at the cell and synapse levels, depended on the duration of the pre-pulse. The time constant (τ) was 1.61 s for maximal $I_{NMDA\text{-}K}$ enhancement by a pre-depolarization from −80 to +40 mV, and 1.97 s for maximal inhibition by a pre-hyperpolarization from +40 mV to −80 mV (both were assessed with a 1 s time gap between the termination of the pre-pulse and the beginning of NMDA application). This time-dependent phenomenon suggests that a few seconds of membrane depolarization or hyperpolarization are sufficient to selectively alter the behaviour of NMDA receptors (Fig. 6). NMDA receptor plasticity was also subject to a time-dependent decay. Increasing the latency between the end of the single depolarizing pulse and the beginning of NMDA application from 1 to 5 s diminished

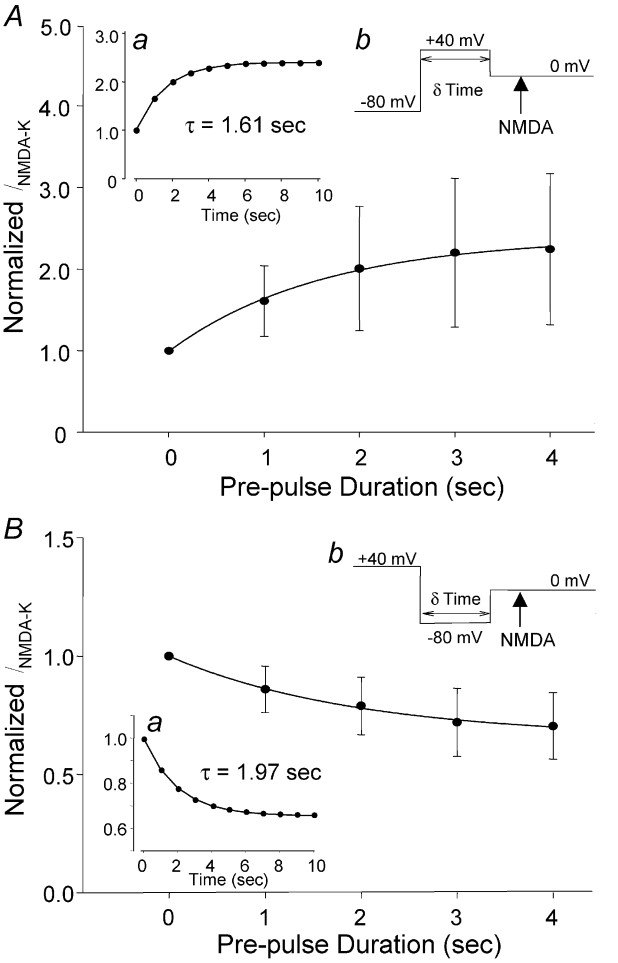

Figure 6. Time-dependent regulation of $I_{NMDA\text{-}K}$

A, the depolarizing pre-pulse-induced upregulation of the isolated $I_{NMDA\text{-}K}$ depended upon the duration of the pre-pulse. Longer pre-pulses from −80 to +40 mV induced larger enhancement of $I_{NMDA\text{-}K}$. Exponential curve fitting (*a*) of the duration (*b*) gave an approximate time constant of 1.61 s for the required duration of pre-depolarization. The single exponential decay equation $I_t = I_0 e^{-t}\tau$ was used for the analysis (SigmaPlot, SPSS, Chicago, IL, USA), where I_t and I_0 were the normalized amplitudes of the current at times t and 0 s, respectively. *B*, stepping to the negative potential of −80 from +40 mV revealed an inhibitory effect on $I_{NMDA\text{-}K}$. The time constant for the effect of the hyperpolarizing step was 1.97 s, as determined by exponential curve fitting (*a*). Inset *b* illustrates the voltage protocols used in these experiments; a 1 s delay was applied between terminating the pre-pulse and starting the application of NMDA. Each point represents the results from six cells.

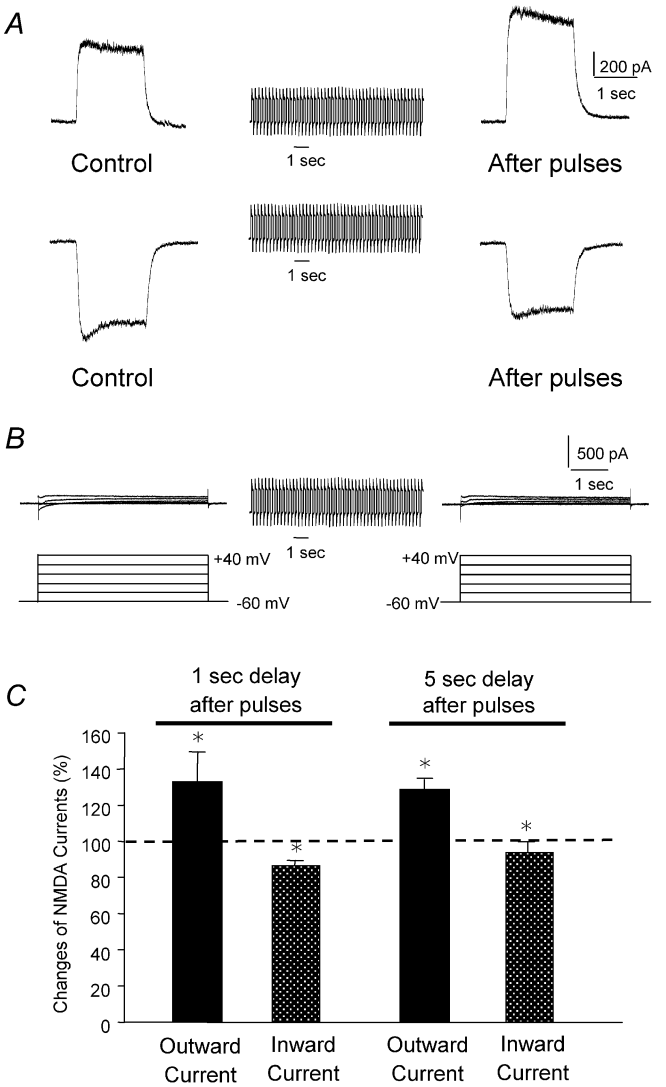

Figure 7. Selective upregulation of $I_{NMDA\text{-}K}$ by a train of brief excitatory pre-pulses

NMDA inward and outward currents were recorded in the same cells and the same solutions at −40 and +40 mV, respectively. A burst of depolarizing pulses (100 ms pulses from −40 to +40 mV at 5 Hz for 10 s) was applied and completed 1 s before NMDA applications. *A*, representative traces of NMDA inward current and outward currents before and after the pre-pulses in the same cell. The outward current was enhanced following one burst of pre-pulses, whereas the inward current decreased. *B*, membrane responses induced by the voltage steps from the holding potential of −60 up to +40 mV remained constant after the train of stimuli. Adding 2 μM Gd^{3+} suppressed the initial inward shifts and induced no other effect (data not shown, but see similar results in Fig. 4*Ad*). *C*, increased NMDA outward current and decreased NMDA inward current recorded with a 1 or 5 s delay after the repetitive depolarizing spikes. The membrane potential was kept at −60 mV between the trials and during the 1 or 5 s delay time. Currents were compared with their controls (dashed line) before the depolarizing pulses and are expressed as a percentage of the control value (n = 15 and 14 for the 1 and 5 s delay, respectively). * Significantly different from controls before pre-pulses ($P < 0.05$).

the pre-conditioning effect; the ratio of $I_{NMDA\text{-}K}$ ($I_{\text{pre-step to +40 mV}}/I_{\text{pre-step to −80 mV}}$) was 1.08 ± 11 ($n$ = 6, $P > 0.05$; but see below for a more persistent modulation after a train of pre-pulses).

In addition to the constant single membrane depolarization, a train of brief pre-pulses (10 s train duration at 5 Hz), as used in long-term potentiation (LTP) studies, similarly triggered the delayed selective augmentation of $I_{NMDA\text{-}K}$ (Fig. 7). In experiments with physiological solutions, NMDA inward and outward currents were recorded in the same cells at holding potentials of −40 and +40 mV, respectively. Following a burst of excitatory activity, the NMDA outward current was noticeably enlarged (Fig. 7). In contrast to the outward current, the NMDA inward current recorded in these cells declined after the train stimulation (Fig. 7). The changes in NMDA currents were unlikely to be caused by contamination of voltage-gated currents. In the presence of voltage-gated channel blockers in the external solution (2 μM Gd^{3+} and 0.5 μM TTX) and internal solution (10 mM TEA and 120 mM Cs^{+}), the voltage-activated membrane responses were small, and their size and shape remained constant after either a single pre-pulse or a train of 10 s stimuli (Fig. 7). Furthermore, a similar selective upregulation of $I_{NMDA\text{-}K}$ was observed even when the time gap between the termination of the train pulses and the beginning of NMDA application was extended to 5 s (Fig. 7*C*). This 5 s delay probably exceeded the deactivation time course of voltage-gated channels in mammalian cells and essentially eliminated their contribution to the modulation of $I_{NMDA\text{-}K}$. The more enduring modulation compared with the short-lasting (< 5 s) modulation following a single pulse (see Fig. 6) is consistent with the activity-dependent feature of $I_{NMDA\text{-}K}$.

As a further confirmation of the voltage- and excitatory activity-dependent modulation of NMDA currents, we next examined the effects of depolarizing spikes during NMDA receptor activation. Since NMDA inward and outward currents could be recorded at an identical holding potential of −10 mV in normal and Na^{+}-free external solutions, respectively, the same pulses depolarizing from −10 to +50 mV at 16–18 Hz for 1 s were applied during the course of a 3 s NMDA application. As expected, the brief depolarizing spikes suppressed the NMDA inward current (27 ± 8 % decrease, n = 4, $P < 0.05$), whereas they increased the outward current (43 ± 9 % increase, n = 6, $P < 0.05$; Fig. 8). This result indicates that the NMDA receptor K^{+} permeability was subject to voltage- and activity-dependent selective regulation even when the receptor channels were in their open state.

DISCUSSION

The present study provides novel evidence that $I_{NMDA\text{-}K}$ exhibits unique characteristics that are different from the

inward current carried by Na^+ and Ca^{2+} through the same channels. Specifically, the NMDA receptor-mediated K^+ efflux is much less sensitive to the well-known desensitization/inactivation of the NMDA receptor induced primarily by accumulation of intracellular Ca^{2+}. As would be expected from this selective regulation of ion permeability, the ratio of inward/outward currents undergoes a time-dependent decrease, and the reversal potential of the composite NMDA current shifted towards negative potentials. Moreover, we revealed that the NMDA receptor K^+ conductance is regulated by a prior membrane potential/activity-dependent mechanism, providing a novel plasticity model at the receptor level. It appears that these observations cannot be explained by the conventional knowledge of NMDA receptor regulation. Collectively, consistent results support our hypothesis that the K^+ permeability of NMDA receptors is under a unique Ca^{2+}-independent, but voltage- and excitatory activity-dependent regulation.

NMDA receptor-mediated K^+ efflux

Previous studies have shown that L-glutamate and NMDA stimulate cellular K^+ loss; extracellular K^+ could increase to 60 mM in just a few minutes (Harvey, 1968; Buhrle & Sonnhof, 1983; Lackington & Orrego, 1986). A number of studies have shown that the permeability of NMDA receptors to K^+ is at least equal to, if not higher than, that to Na^+ (Jan & Jan, 1976; Anwyl, 1977; Matthews & Wickelgren, 1979; Dekin, 1983; Mayer & Westbrook, 1987*b*; Ascher & Nowak, 1988; Ozawa *et al.* 1988; Chang *et al.* 1994). A permeability to K^+ that is about 1.1-fold higher than that to Na^+ was also demonstrated in the cloned NR1/NR2 receptor channels (Tsuzuki *et al.* 1994). It seems necessary to point out that the K^+ efflux through NMDA receptor channels is not an event that takes place in the absence of Ca^{2+} and Na^+; it occurs simultaneously with influx Ca^{2+} and Na^+ into the cell and at similar physiological membrane potentials. This conclusion is evidenced by the fact that composite NMDA receptor currents normally have a reversal potential around 0 mV, in accordance with the calculated Nernst potentials for Ca^{2+}, Na^+ and K^+ (Mayer & Westbrook, 1987*b*). The fact that stimulation of NMDA receptors can significantly reduce intracellular K^+, either in normal conditions (Harvey, 1968; Buhrle & Sonnhof, 1983; Lackington & Orrego, 1986) or under conditions mimicking the ischaemic brain (Yu *et al.* 1999*a*), suggests the importance of NMDA receptor-mediated K^+ efflux in K^+ homeostasis,

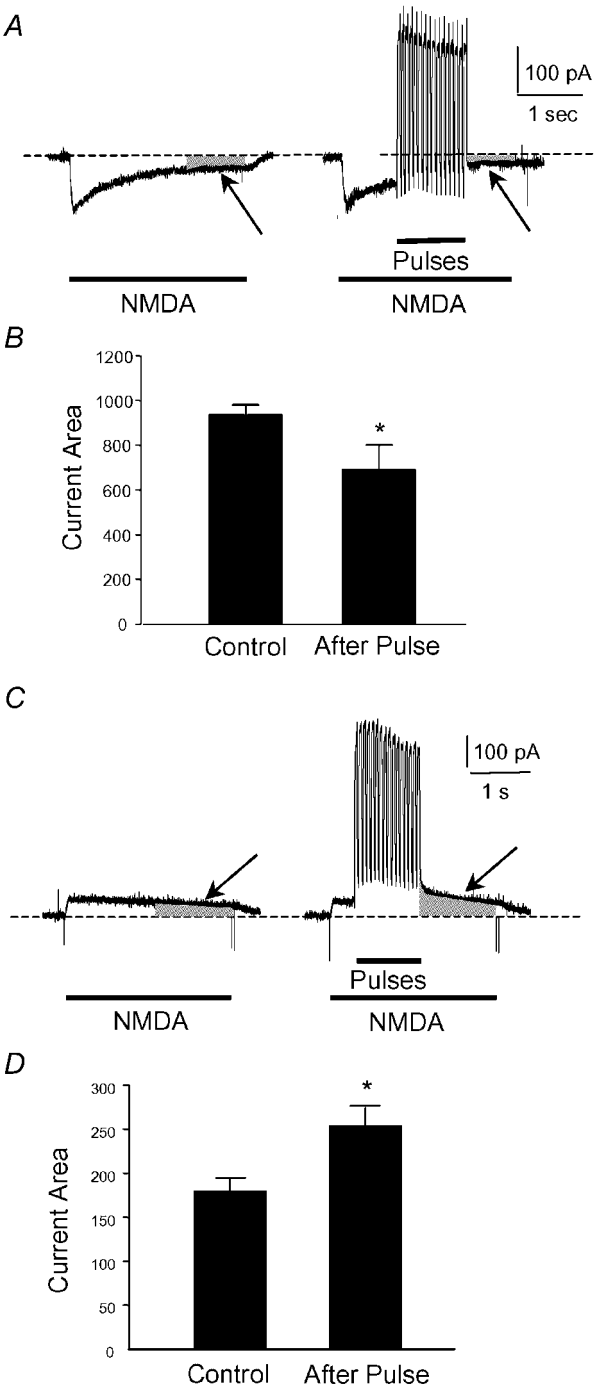

Figure 8. Voltage- and activity-dependent regulation of I_{NMDA} during NMDA receptor activation

NMDA inward and outward currents were recorded in different cells in normal and Na^+-free external solutions, respectively. The concentration of Ca^{2+} was normal (2 mM) in both solutions. Since NMDA currents of opposite directions could be recorded at the identical membrane potential of −10 mV, the same depolarizing pulses (from −10 to +50 mV at 16–18 Hz for 1 s were applied during the 3 s NMDA application. Current area (see the shaded areas in *A* and *B* indicated by the arrows) was measured to reflect the time-dependent changes. *A*, the depolarizing pulses facilitated the desensitization of the NMDA inward current. The bar graph in *B* shows the significant reduction in the current area after the pulses compared with the corresponding current area of the control current ($n = 4$). *C*, the same depolarizing stimuli augmented the NMDA outward current compared with the corresponding control current area. The bar graph in *D* shows the control and enhanced current area during the period following depolarizing pulses ($n = 6$). The bar values in *B* and *D* are arbitrary numbers. * Significantly different from controls.

which may have a vital impact on membrane excitability and the intracellular events related to apoptosis (Dallaporta *et al.* 1998; Bortner & Cidlowski, 1999; Yu, 2003).

The lack of Ca^{2+} sensitivity of $I_{NMDA\text{-}K}$

The outward $I_{NMDA\text{-}K}$ showed much less sensitivity to the level of $[Ca^{2+}]_i$ than the NMDA inward current. This is surprising given current knowledge about NMDA receptor regulation; ironically, supporting evidence can be found in previously published works. Vyklicky (1993) reported that the NMDA outward current remained stable following the conditioning stimulation of 100 μM NMDA applied at 0.5 Hz, which normally induces enhanced desensitization of the NMDA inward current. Unfortunately, no further investigation of this phenomenon has been carried out, perhaps because of the popular perception that the K^+ permeability of NMDA receptors has little, if any, physiological or pathological significance, and that ion movements through a receptor channel are similarly regulated.

The different Ca^{2+} sensitivity of ion movements via NMDA receptors can be clearly demonstrated by the isolated inward and outward currents. More importantly, when Na^+ influx is diminished, the difference can be revealed by recordings at the same Ca^{2+} concentration and identical membrane potential. Since extracellular Na^+ may reduce the affinity of NMDA receptor agonists to their binding site or reduce the Mg^{2+} association rate constant (Yoneda & Ogita, 1991; Zhu & Auerbach, 2001), it might be argued that the stable outward current in our experiments could be attributed to the lack of extracellular Na^+. Although we cannot completely rule out a role for Na^+ in the modulation of the outward current, this possibility is not supported by the shift in the reversal potential of composite NMDA receptor currents recorded in physiological solutions with normal Na^+ concentrations. On the other hand, decreased Na^+ influx or a lower intracellular Na^+ concentration may downregulate NMDA receptor activities (Yu & Salter, 1998); this mechanism apparently cannot be linked to the lack of rundown of $I_{NMDA\text{-}K}$. Our data rather suggest that the K^+ efflux via NMDA receptors is not subject to the previously reported downregulation by a lower intracellular Na^+ concentration or lack of Na^+.

We have demonstrated that the selective upmodulation of $I_{NMDA\text{-}K}$ by prior depolarization/excitatory activity could be observed in a Ca^{2+}-free solution or when Ca^{2+} influx is blocked. Thus, it appears that not only was $I_{NMDA\text{-}K}$ insensitive to changes in $[Ca^{2+}]_i$, the voltage- and activity-dependent modulation of $I_{NMDA\text{-}K}$ was also Ca^{2+} independent.

Consistent with differential regulation of NMDA inward and outward conductances, the reversal potential of NMDA composite currents shifted towards negative values. At first glance, the −8.5 mV shift in the reversal potential may not seem so striking; this may in fact partly explain why this phenomenon has been overlooked in previous investigations. On the other hand, among the three permeable cations, K^+ is the only one with a negative equilibrium potential; both Ca^{2+} and Na^+ have very positive equilibrium potentials. This implies that even a small negative shift must represent significant alterations in the relative permeability of these three cations. This was exemplified by the striking difference in the rundown behaviour between the inward and outward currents and the large change in the ratio of inward/outward currents observed in our experiments (Figs 2 and 3).

Structural homology between voltage-gated K^+ channels and NMDA receptor channels

There is a striking degree of amino acid homology across the pore-forming regions of voltage-gated K^+ channels and glutamate receptors (Wood *et al.* 1995). Other ligand-gated channels, including the acetylcholine, GABA, glycine and serotonin receptors, show much weaker homology with K^+ channels (Wood *et al.* 1995). The pore-forming M2 segment of the NMDA NR1 subunit forms a hairpin structure similar to that found in K^+ channels. Structural similarities were identified between the C-termini of NR2A/2B subunits and K^+ channels (Niethammer *et al.* 1996). The idea of structural conservation between K^+ channels and glutamate receptor channels was supported recently by the discovery of the novel GluR0 receptor (Chen *et al.* 1999). Although compelling evidence suggests that the K^+ permeability of NMDA receptors is inherited from voltage-gated K^+ channels, there is so far no functional implication of these structural similarities. The voltage-dependent modulation of the K^+ permeability of NMDA receptor channels may shed light on the functional link between these channels.

Modulation of NMDA receptor channels by prior membrane potential and activity: hysteresis *vs.* voltage–activity-dependent preconditioning (receptor plasticity)

Membrane depolarization activates voltage-gated channels that might interfere with or even contribute to the voltage-dependent regulation. The enhancement of the NMDA outward current by prior membrane depolarization persisted in the presence of the Ca^{2+} channel antagonists gadolinium or nifedipine and the Na^+ channel blocker TTX, suggesting that voltage-gated Ca^{2+} channels and Na^+ channels did not contribute to the observed modulation. Conditions such as K^+-free internal solution and TEA were used to eliminate activation of voltage-gated K^+ channels. The most abundant K^+ channels with high K^+ conductance in cortical neurons are the outward, delayed rectifier I_K channels. These channels are deactivated upon repolarization, with a time constant of 2–20 ms (Dale, 1995). The K^+ channels linking to prolonged influence of voltage-induced Ca^{2+} influx are the I_{AHP} channels or

apamin-sensitive/-insensitive SK_{Ca} channels, which have a deactivating time constant of 1–2 s (Sah, 1996). The SK_{Ca} current may also be activated following NMDA receptor activation; however, a very high concentration of NMDA (1 mM) is required and, again, this SK_{Ca} current delays with a time constant of 1.4 s (Shah & Haylett, 2002). Since the voltage–activity-preconditioning effect was observed even 5 s after the termination of the train stimuli, it is unlikely that voltage-gated and Ca^{2+}-activated K^+ channels play any significant role in enhancing $I_{NMDA\text{-}K}$. Of great relevance, we also showed that voltage-activated membrane current responses remained small and stable under our experimental conditions.

Nowak & Wright (1992) reported that voltage-dependent hysteresis of the NMDA current *I–V* curves developed after membrane potential changes. The voltage- and activity-enhanced $I_{NMDA\text{-}K}$ observed in our study, however, is obviously different from the hysteresis previously described in a number of aspects. The voltage-preconditioning effect on outward current developed much faster (τ = 1–2 s compared with 2–14 min for hysteresis to reach its equilibrium state). Furthermore, the hysteresis showed enhancing effects on both the inward and outward currents, whereas the voltage-preconditioning in our study selectively enhanced the outward current only, as demonstrated with either isolated $I_{NMDA\text{-}K}$ or composite NMDA currents in physiological solutions. Moreover, we showed that prior membrane depolarization and hyperpolarization had opposite effects on $I_{NMDA\text{-}K}$. Therefore, the voltage–activity preconditioning represents a faster and more dynamic form of NMDA receptor modulation or a novel form of receptor plasticity, which is mediated by a mechanism that is distinct from hysteresis.

Does the NMDA receptor plasticity have any significant role in physiological and pathological conditions? The brief pulses used in the experiment shown in Fig. 7 depolarized the membrane to +40 mV, which is within or near the range reached by action potentials. Similar, or much longer stimulations (i.e. 20 s bursts of 100 ms pulses at 5 Hz) have been used in LTP investigations (Alonso *et al.* 1990). Interestingly, transient increases in extracellular K^+ concentration, probably mediated by NMDA receptors, could cause or facilitate the generation of LTP (Ballyk & Goh, 1992; Fleck *et al.* 1992; Bernard *et al.* 1994). It is conceivable that the selective upregulation of $I_{NMDA\text{-}K}$ could provide a putative mechanism contributing to the K^+-associated generation and/or modulation of LTP. We are currently investigating the possible influence of $I_{NMDA\text{-}K}$ regulation on LTP. It is also possible that more optimized excitatory stimuli may boost $I_{NMDA\text{-}K}$ modulation. Even more vigorous activities may develop in pathological situations like epilepsy (Ebersole & Levine, 1975; Bragin *et al.* 1999). Prolonged depolarization for many seconds or even minutes occurs during and after brain ischaemia (Nedergaard & Hansen, 1993). Because of the pro-apoptotic effect of NMDA receptor-mediated K^+ efflux, we suggest that the selective upregulation of $I_{NMDA\text{-}K}$ induced by prior depolarization and by membrane excitatory activities plays an important role in the pathogenesis of certain disease states, particularly in conditions involving excessive glutamate release, decreased glutamate uptake, depolarized membrane potentials and insufficient energy supply.

REFERENCES

Alonso A, De Curtis M & Llinas R (1990). Postsynaptic Hebbian and non-Hebbian long-term potentiation of synaptic efficacy in the entorhinal cortex in slices and in the isolated adult guinea pig brain. *Proc Natl Acad Sci U S A* **87**, 9280–9284.

Anwyl R (1977). Permeability of the post-synaptic membrane of an excitatory glutamate synapse to sodium and potassium. *J Physiol* **273**, 367–388.

Ascher P & Nowak L (1988). The role of divalent cations in the N-methyl-D-aspartate responses of mouse central neurones in culture. *J Physiol* **399**, 247–266.

Ballyk BA & Goh JW (1992). Elevation of extracellular potassium facilitates the induction of hippocampal long-term potentiation. *J Neurosci Res* **33**, 598–604.

Bernard J, Lahsaini A & Massicotte G (1994). Potassium-induced long-term potentiation in area CA1 of the hippocampus involves phospholipase activation. *Hippocampus* **4**, 447–453.

Bortner CD & Cidlowski JA (1999). Caspase independent/dependent regulation of K^+, cell shrinkage, and mitochondrial membrane potential during lymphocyte apoptosis. *J Biol Chem* **274**, 21953–21962.

Bragin A, Engel J Jr, Wilson CL, Fried I & Mathern GW (1999). Hippocampal and entorhinal cortex high-frequency oscillations (100–500 Hz). in human epileptic brain and in kainic acid-treated rats with chronic seizures. *Epilepsia* **40**, 127–137.

Buhrle CP & Sonnhof U (1983). The ionic mechanism of the excitatory action of glutamate upon the membranes of motoneurones of the frog. *Pflugers Arch* **396**, 154–162.

Burnashev N, Schoepfer R, Monyer H, Ruppersberg JP, Gunther W, Seeburg PH & Sakmann B (1992). Control by asparagine residues of calcium permeability and magnesium blockade in the NMDA receptor. *Science* **257**, 1415–1419.

Chang H, Ciani S & Kidokoro Y (1994). Ion permeation properties of the glutamate receptor channel in cultured embryonic *Drosophila* myotubes. *J Physiol* **476**, 1–16.

Chen GQ, Cui C, Mayer ML & Gouaux E (1999). Functional characterization of a potassium-selective prokaryotic glutamate receptor. *Nature* **402**, 817–821.

Choi DW (1992). Excitotoxic cell death. *J Neurobiol* **23**, 1261–1276.

Dale N (1995). Kinetic characterization of the voltage-gated currents possessed by *Xenopus* embryo spinal neurons. *J Physiol* **489**, 473–488.

Dallaporta B, Hirsch T, Susin SA, Zamzami N, Larochette N, Brenner C, Marzo I & Kroemer G (1998). Potassium leakage during the apoptotic degradation phase. *J Immunol* **160**, 5605–5615.

Dekin MS (1983). Permeability changes induced by L-glutamate at the crayfish neuromuscular junction. *J Physiol* **341**, 105–125.

Ebersole JS & Levine RA (1975). Abnormal neuronal responses during evolution of a penicillin epileptic focus in cat visual cortex. *J Neurophysiol* **38**, 250–256.

Fleck MW, Palmer AM & Barrionuevo G (1992). Potassium-induced long-term potentiation in rat hippocampal slices. *Brain Res* **580**, 100–105.

Gibb AJ & Colquhoun D (1992). Activation of *N*-methyl-D-aspartate receptors by L-glutamate in cells dissociated from adult rat hippocampus. *J Physiol* **456**, 143–179.

Harvey AMH (1968). Excitatory acidic amino acids and the cation content and sodium ion flux of isolated tissues from the brain. *Biochem J* **108**, 269–274.

Hollmann M & Heinemann S (1994). Cloned glutamate receptors. *Annu Rev Neurosci* **17**, 31–108.

Ichinose T & Yu SP (2000). Unique regulation of the K^+ current mediated by NMDA receptor channel in mouse cortical neurons. *Soc Neurosci Abstr* **26**, 2147.

Inai Y, Yabuki M, Kanno T, Akiyama J, Yasuda T & Utsumi K (1997). Valinomycin induces apoptosis of ascites hepatoma cells (AH-130) in relation to mitochondrial membrane potential. *Cell Struct Funct* **22**, 555–563.

Jan LY & Jan YN (1976). L-glutamate as an excitatory transmitter at the *Drosophila* larval neuromuscular junction. *J Physiol* **262**, 215–236.

Jatzke C, Watanabe J & Wollmuth LP (2002) Voltage and concentration dependence of Ca^{2+} permeability in recombinant glutamate receptor subtypes. *J Physiol* **538**, 25–39.

Lackington I & Orrego F (1986). Continuous measurement of net potassium movements in rat brain cortex suspensions. Effects of glutamate, veratridine, creatine and other substances. *Brain Res* **378**, 390–393.

Legendre P, Rosenmund C & Westbrook GL (1993). Inactivation of NMDA channels in cultured hippocampal neurons by intracellular calcium. *J Neurosci* **13**, 674–684.

McCarthy JVCTG (1997). Cell shrinkage and apoptosis: a role for potassium and sodium ion efflux. *Cell Death Differ* **4**, 756–770.

MacDermott AB, Mayer ML, Westbrook GL, Smith SJ & Barker JL (1986). NMDA-receptor activation increases cytoplasmic calcium concentration in cultured spinal cord neurones. *Nature* **321**, 519–522.

Matthews G & Wickelgren WO (1979). Glutamate and synaptic excitation of reticulospinal neurones of lamprey. *J Physiol* **293**, 417–433.

Mayer ML, Vyklicky L Jr & Clements J (1989). Regulation of NMDA receptor desensitization in mouse hippocampal neurons by glycine. *Nature* **338**, 425–427.

Mayer ML & Westbrook GL (1987*a*). The physiology of excitatory amino acids in the vertebrate central nervous system. *Prog Neurobiol* **28**, 197–276.

Mayer ML & Westbrook GL (1987*b*). Permeation and block of N-methyl-D-aspartic acid receptor channels by divalent cations in mouse cultured central neurones. *J Physiol* **394**, 501–527.

Mayer ML, Westbrook GL & Guthrie PB (1984). Voltage-dependent block by Mg^{2+} of NMDA responses in spinal cord neurones. *Nature* **309**, 261–263.

Medina I, Filippova N, Charton G, Rougeole S, Ben-Ari Y, Khrestchatisky M & Bregestovski P (1995). Calcium-dependent inactivation of heteromeric NMDA receptor-channels expressed in human embryonic kidney cells. *J Physiol* **482**, 567–573.

Monaghan DT, Bridges RJ & Cotman CW (1989). The excitatory amino acid receptors: their classes, pharmacology, and distinct properties in the function of the central nervous system. *Annu Rev Pharmacol Toxicol* **29**, 365–402.

Nedergaard M & Hansen AJ (1993). Characterization of cortical depolarizations evoked in focal cerebral ischemia. *J Cereb Blood Flow Metab* **13**, 568–574.

Niethammer M, Kim E & Sheng M (1996). Interaction between the C terminus of NMDA receptor subunits and multiple members of the PSD-95 family of membrane-associated guanylate kinases. *J Neurosci* **16**, 2157–2163.

Nowak LM & Wright JM (1992). Slow voltage-dependent changes in channel open-state probability underlie hysteresis of NMDA responses in Mg^{2+}-free solutions. *Neuron* **8**, 181–187.

Ozawa S, Nakamura T & Yuzaki M (1988). Cation permeability change caused by L-glutamate in cultured rat hippocampal neurons. *Brain Res* **443**, 85–94.

Rosenmund C, Feltz A & Westbrook GL (1995). Calcium-dependent inactivation of synaptic NMDA receptors in hippocampal neurons. *J Neurophysiol* **73**, 427–430.

Rosenmund C & Westbrook GL (1993). Rundown of N-methyl-D-aspartate channels during whole-cell recording in rat hippocampal neurons: role of Ca^{2+} and ATP. *J Physiol* **470**, 705–729.

Rothman SM & Olney JW (1986). Glutamate and the pathophysiology of hypoxic-ischemic brain damage. *Ann Neurol* **19**, 105–111.

Sah P (1996). Ca^{2+}-activated K^+ currents in neurones: types, physiological roles and modulation. *Trends Neurosci* **19**, 150–154

Shah MM & Haylett DG (2002). K^+ currents generated by NMDA receptor activation in rat hippocampal pyramidal neurons. *J Neurophysiol* **87**, 2983–2989

Schneggenburger R (1998). Altered voltage dependence of fractional Ca^{2+} current in N-methyl-D-aspartate channel pore mutants with a decreased Ca^{2+} permeability. *Biophys J* **74**, 1790–1974.

Schneggenburger R & Ascher P (1997). Coupling of permeation and gating in an NMDA-channel pore mutant. *Neuron* **18**, 167–177.

Tikhonov DB, Zhorov BS & Magazanik LG (1999). Intersegment hydrogen bonds as possible structural determinants of the N/Q/R site in glutamate receptors. *Biophys J* **77**, 1914–1926.

Tsuzuki K, Mochizuki S, Iino M, Mori H, Mishina H & Ozawa S (1994). Ion permeation properties of the cloned mouse epsilon 2/zeta 1 NMDA receptor channel. *Brain Res Mol Brain Res* **26**, 37–46.

Vyklicky L Jr (1993). Calcium-mediated modulation of N-methyl-D-aspartate (NMDA) responses in cultured rat hippocampal neurones. *J Physiol* **470**, 575–600.

Watkins JC & Evans RH (1981). Excitatory amino acid transmitters. *Annu Rev Pharmacol Toxicol* **21**, 165–204.

Wilson WA & Goldner MM (1975). Voltage clamping with a single microelectrode. *J Neurobiol* **6**, 411–422.

Wood MW, Vandongen HM & Vandongen AM (1995). Structural conservation of ion conduction pathways in K channels and glutamate receptors. *Proc Natl Acad Sci U S A* **92**, 4882–4886.

Wright JM, Kline PA, & Nowak LM (1991) Multiple effects of tetraethylammonium on N-methyl-D-aspartate receptor-channels in mouse brain neurons in cell culture. *J Physiol* **439**, 579–604.

Xiao AY, Homma M, Wang XQ, Wang X & Yu SP (2001). Role of K^+ efflux in apoptosis induced by AMPA and kainate in mouse cortical neurons. *Neuroscience* **108**, 61–67.

Yoneda Y & Ogita K (1991). Inhibitory modulation by sodium ions of the N-methyl-D-aspartate recognition site in brain synaptic membranes. *J Neurochem* **57**, 2036–2046.

Yu SP (2003). Regulation and critical role of potassium homeostasis in apoptosis. *Prog Neurobiol* (in press). DOI: 10.1016/S0301-0082(03)00090-X

Yu SP & Ichinose T (1999). The potassium current mediated by NMDA receptor channels in cortical neurons. *Soc Neurosci Asbtr* **25**, 1485.

Yu SP, Yeh CH, Gottron F, Wang X, Grabb MC & Choi DW (1999*b*). Role of the outward delayed rectifier K^+ current in ceramide-induced caspase activation and apoptosis in cultured cortical neurons. *J Neurochem* **73**, 933–941.

Yu SP, Yeh CH, Sensi SL, Gwag BJ, Canzoniero LM, Farhangrazi ZS, Ying HS, TiaN, M, Dugan LL & Choi DW (1997). Mediation of neuronal apoptosis by enhancement of outward potassium current. *Science* **278**, 114–117.

Yu SP, Yeh CH, Strasser U, Tian M & Choi DW (1999*a*). NMDA receptor-mediated K^+ efflux and neuronal apoptosis. *Science* **284**, 336–339.

Yu XM & Salter MW (1998). Gain control of NMDA-receptor currents by intracellular sodium. *Nature* **396**, 469–474.

Zhu Y & Auerbach A (2001). Na^+ occupancy and Mg^{2+} block of the N-methyl-D-aspartate receptor channel. *J Gen Physiol* **117**, 275–286.

Acknowledgements

This work was supported by grants from National Institute of Health (NS42236), the National Science Foundation (9817151) and the American Heart Association (0170064N).